Published in final edited form as:
J Mater Chem. 2010 January 1; 20(3): 547–554. doi:10.1039/b913224d.

Fabrication and functional characterization of goldnanoconjugates for potential application in ovarian cancer

Chitta Ranjan Patra[1], **Resham Bhattacharya**[1], and **Priyabrata Mukherjee**[1,2,*]

[1]Department of Biochemistry and Molecular Biology, 200 First Street SW, Mayo Clinic, Rochester, MN 55905

[2]Department of Biomedical Engineering, 200 First Street SW, Mayo Clinic, Rochester, MN 55905

Abstract

In this paper we report the surface modification and functional characterization of a gold nanoparticle-based drug delivery system for potential therapeutic application in ovarian cancer. It is currently recognized that nanotechnology may play a pivotal role in drug delivery by increasing efficacy and reducing toxicity of anti-cancer drugs. Here, we report the fabrication of a gold nanoparticles (AuNP) based drug delivery system consisting of folic acid (FA), mercapto-polyethylene glycol (PEG-SH) with a molecular weight of 2000 (designated as PSH2-2K or PSH) and cis-platin (CP) [Au-PSH-CP-FA] for potential therapeutic application in ovarian cancer. Fabrication is done in a three steps incubation process at room temperature (RT). The gold nanoconjugates are characterized with several physico-chemical techniques such as UV-Vis (UV-Visible spectroscopy), TEM (Transmission electron microscopy), ICP (Inductively coupled plasma) and radioactivity measurement with a scintillation counter. Attachment and release profiles of FA from the gold nanoconjugates are performed using ^{3}H-labelled FA (^{3}H-FA). The expressions of folate receptor (FR) for ovarian cancer cell lines (OV-167, OVCAR-5), human umbilical vein endothelial cells (HUVEC) and ovarian surface epithelial (OSE) cells are determined by FACS analysis. Quantitation of platinum content in the nanoconjugates and its release profile is determined by platinum (Pt) analysis using ICP-MS. Biological functional characterization using *in vitro* proliferation assay demonstrates that Au-PSH-CP-FA not only retains the cytotoxic effect of CP, but it protects the normal cells from the cytotoxic insult, while enhancing the cytotoxic effect on the tumor cells. In future, this strategy may be utilized as a strategy for the treatment of ovarian cancers and may overcome the core side effect issues in anticancer therapy.

Keywords

Gold nanoparticles; Cis-platin; Folic acid; Ovarian Cancer; Drug Delivery

INTRODUCTION

Cancer is one of the leading causes of morbidity and mortality in the United States. Ovarian cancer is one of the fourth most common cancers among women, and it is one of the major leading causes of deaths than any other type of female reproductive cancer in the United States.[1-5] Approximately 22,000 new cases of ovarian cancer are diagnosed each year and 16,000 per year die from this disease. Ovarian cancer is often called the “silent killer” because symptoms

*Address for correspondence: Priyabrata Mukherjee, Ph.D, Department of Biochemistry and Molecular Biology, Department of Biomedical Engineering, 200 First Street SW, Mayo Clinic, Rochester, MN-55905, USA, mukherjee.priyabrata@mayo.edu, Phone: 507-284-8563, Fax: 507-293-1058.

observed in the early stages are not easily connected to the disease. [1, 2, 6] Ovarian cancers are usually treated by surgery, radiation therapy, chemotherapy or a combination of treatments etc. Surgical debulking followed by radiation and chemotherapy are common mode of treatment for all stages of ovarian cancer. However, anticancer drugs are highly toxic and exhibit severe side effects. Therefore, new drug delivery strategies are needed to combat this deadly disease.

Complete remission of cancer without the collateral damage is the ultimate goal of anti-cancer therapy. In this context nanotechnology may play a significant role by increasing the efficacy of the drug, that in turn will reduce the dose and hence the side effects. Various agents such as antibodies, lectins, growth factors, cytokines, hormones, low-density lipoproteins and small molecules such as folic acid, etc, with varying specificity have been used to target different types of cancer, mainly for drug delivery applications. [7-14] It is well established that the FRs are over-expressed in a number of malignant cells including ovarian, kidney, lung, breast, endometrial, colorectal and brain, etc, compared to their normal counterpart. 7-14 Thus, FR targeting has become one of the important approaches for targeted drug delivery in cancer therapy. [15, 16] In the present article we fabricate such a drug delivery system by surface modifying AuNP with CP, PSH and FA. Release profile of CP and FA from Au-PSH-FA-CP demonstrate significant stability of the nanconjugates under physiological salt concentration. Nanoconjugates are physico-chemically characterized mainly by UV-Visible spectroscopy (UV-Vis) and transmission electron microscopy (TEM). Quantification of CP in the nanoconjugates is confirmed by inductively coupled plasma (ICP) analysis. Functional characterizations of the nanoconjugates are tested against the proliferation of OVCAR-5, OV167, HUVECs and OSE. It demonstrates that the nanoconjugates containing FA (Au-PSH-CP-FA) is less toxic to normal ovarian surface epithelium (OSE) and human umbilical vein endothelial cells (HUVECs), whereas, it exhibits higher toxicity to malignant cells compared to Au-PSH-CP and CP only. This strategy may be utilized in future for potential therapeutic application in ovarian cancer and overcome the side effects as these conjugates demonstrate higher toxicity to tumor cells compared to normal cells. [8]

2. MATERIALS AND METHODS

2.1.Materials

Tetrachloroauric acid ($HAuCl_4$), sodium borohydride ($NaBH_4$) and Cis-diamminedichloroplatinum(II) (briefly cis-platin or CP) (99.9%) was purchased from Aldrich Chemicals, St. Louis, USA. Polyethylene glycol disulfhydryl [PEG-$(SH)_2$; F.W =2,000 (designated as PSH2-2K), lot no: C2SH-002-04191] was obtained from the SunBio Corporation USA Office, Orinda, CA. Folic acid (98%) was purchased from Sigma, USA. Tritiated folic acid (^{3}H-FA) was purchased from Amersham Phermaceuticals, UK. [^{3}H] Thymidine was purchased from Amersham Biosciences, Piscataway, NJ. Endotoxin free water was used for synthesis of gold nanoparticle. All the chemicals were used as received without further purification. The human umbilical vein endothelial cells (HUVEC) and its individual components for making endothelial growth medium (EGM) complete media were obtained from Cambrex Bio Science Walkersvile, Inc, MD, USA. Dubelco's Modification of Eagle's Medium (DMEM, 1X) and minimum essential medium (MEM 1x) were purchased from Cellegro, Mediatech, Inc, Herndon, VA, USA.

2.2. Detection of endotoxin in water

The milipore H_2O, used for all experiments in our research was tested for endotoxin using the Gel clot method according to manufacture's instructions (Cat # GS 250Cape Cod Associates, CapeCod). The formation of a gel-clot indicates the presence of endotoxin in a sample. However, we have not found any gel-clot indicating absence of endotoxin in milipore H_2O.

2.3. Preparation of cis-platin (CP) stock solution

A stock solution of cis-platin (10 mg/mL) was prepared by dissolving 10mg of cis-platin in dimethyl sulfoxide (DMSO). Working CP solutions were prepared by diluting the stock solution with PBS to the desired concentration. We use freshly prepared CP stock solution each time for all experiments.

2.4. Standards folic acid (FA) solution

A stock FA solution was prepared by dissolving FA in phosphate buffer solution (PBS) (pH =7.4) to a concentration of 10.0 mg/ml by adding 5 μl of 10(N) NaOH. Working FA standard solutions were prepared by diluting the stock solution with PBS to concentrations within the range of 1–50 μg/ml. We use freshly prepared FA stock solution each time for all experiments.

2.5. Synthesis of gold nanoparticles (AuNPs)

Synthesis of gold nanoparticles (AuNPs) was carried out by the interaction of aqueous solution of $HAuCl_4$ and $NaBH_4$ solution under vigorous stirring in a 2L flask according to our previously reported literature.[15¯18]Initially, a stock solution of $HAuCl_4$ was prepared by dissolving 1g of $HAuCl_4$ in endotoxin free H_2O to a concentration of 10^{-2} (M). Briefly, 10 ml of 10^{-2}(M) $HAuCl_4$ was diluted to 1000 ml with H_2O (endotoxin free) and an aqueous solution of sodium borohydride (~45 mg of $NaBH_4$ in 500 ml of H_2O) was added to it under vigorous stirring and the stirring was continued for 12-16 h to obtain the gold nanoparticles (AuNPs) used in this study.

2.6. Synthesis of AuNPs containing PEG-backbones (Au-PSH)

Gold nanoconjugates (Au-PSH) containing polyethylene glycol disulfhydryl [PEG-$(SH)_2$ (designated as PSH2-2K)] was prepared using a single step incubation by mixing AuNPs solution and PSH2-2k (2.5 μg/mL of AuNPs) under stirring at room temperature. After 1h of incubation, the UV-visible spectra of the resultant solutions were taken to measure the absorbance of gold nanoconjugates. The resulting nanoconjugate solutions were ultra centrifuged at 18,000 rpm for 1h at 10° C in a Sorvall Ultra centrifuge OTD80B using a 502Ti rotor. The resulting loose pellets were collected, lyophilized and used for further chemical characterization as previously reported. [15]

2.7. Synthesis of AuNPs containing PEG-backbones and cis-platin(Au-PSH-CP)

The nanoconjugates containing PSH-2k and cis-platin were prepared by two steps sequential incubation process at room temperature in a similar method as described above. After initial 1h incubation of AuNPs with PSH2-2k molecules, an solution of cis-platin (5 μg/mL of AuNP) dissolved in dimethyl sulfoxide (DMSO) was added to the resultant solution and stirred for another 1h. After the final incubation, the UV-visible spectra of the resultant solutions were taken to measure the absorbance of gold nanoconjugates and the resulting solutions were ultra centrifuged at 18,000 rpm for 1h at 10° C as described above. The resulting loose pellets were collected, lyophilized and used for further chemical characterization. Amount of cis-platin was determined by ICP-MS instrument.

2.8. Synthesis of AuNPs containing PEG-backbones, cis-platin and folic acid (Au-PSH-CP-FA)

The gold nanoconjugates (Au-PSH-CP-FA) containing PSH2-2k, CP and FA were prepared by three steps sequential incubation process at room temperature in a similar method as described above. After initial sequential incubation of AuNPs with PSH2-2k and CP for 1h each as described above, an aqueous solution of folic acid (5 μg /ml) in PBS was added to the resultant solution and stirred for another 1h. After the final incubation, the UV-visible spectra

of the resultant solutions were taken to measure the absorbance of gold nanoconjugates and the resulting solutions were purified by ultra centrifugation at 18,000 rpm for 1h at 10° C and processed as described above.

2.9. Attachment and quantification of radio labeled folic acid (^{3}H-FA) from Au-PSH-CP-(^{3}H-FA)

The gold nanoconjugates (Au-PSH-CP-^{3}H-FA) containing PSH2-2k, cis-platin and ^{3}H-FA (instead of non labeled FA) were prepared by three steps incubation process at room temperature in a similar method as described above (section 2.8). In this case, gold nanoconjugates Au-PSH2-CP as prepared above were treated with 1μCi/ml of ^{3}H-FA (instead of non-labeled FA) and stirred for 1 h. After the final incubation step, the resulting solutions were then centrifuged at 40,000 rpm at 10 °C for 1h in a Beckman TL-100 ultracentrifuge using a TLA-100.2 rotor. The loose pellets and the clear supernatant were collected and measured for radioactivity using a scintillation counter to determine the amount of ^{3}H-FA in goldnanoconjugates. The radioactivity measurement was also used to study the release profile of ^{3}H-FA in PBS from the conjugates.

2.10. Cell culture experiments

OVCAR-5 and OV-167 cells (Ovarian cancer cells) were cultured using DMEM and MEM complete media supplemented with 10% fetal bovine serum, 5% L-Glutamine, and 1% antibiotics, respectively. HUVECs were cultured in EGM media containing10% fetal bovine serum and ovarian surface epithelial (OSE) cells were grown in OSE media containing 15% fetal bovine serum. All Cells were maintained at 37°C in an atmosphere containing 95% air-5% CO2 (v/v).

2.11. Proliferation experiments using ^{3}H-Thymidine incorporation assay

Briefly, 2×10^4 of all type cell lines (HUVEC, OSE, OVCAR-5, OV-167) were seeded in 24-well plates, cultured for 1 day in corresponding complete media, followed by treatment with different doses of free CP, and nanoconjugated CP (Au-PSH-CP and Au-PSH-CP-FA) for 2h. After the treatment cells were washed with their respective media and incubated in the humidified chamber for another 20 hours. Following the final incubation, 1 μCi [^{3}H] thymidine in cell growth media was added to each well. Four hours later, cells were washed with cold PBS, fixed with 100% cold methanol, and collected for the measurement of trichloroacetic acid–precipitable radioactivity. Experiments were repeated in triplicate.

3. CHARACTERIZATION

Gold nanoparticles (AuNPs) and its nanoconjugates (Au-PSH, Au-PSH-CP, Au-PSH-CP-FA) were characterized using UV-Visible spectroscopy, transmission electron microscopy (TEM) and inductively coupled plasma (ICP) analysis as previous described.[15, 19, 20]

The concentration of CP in gold nanoconjugates (Au-PSH-CP and Au-PSH-CP-FA) was measured by quantifying platinum content using inductively coupled plasma analysis as previously reported. [15] A series of standard solution of CP was prepared and the response factor was calculated by measuring the amount of CP in standard solution using ICP-MS. Similarly, we have quantified the CP content in gold nanoconjugates (Au-PSH-CP and Au-PSH-CP-FA) using ICP-MS. Each experiment was repeated for three times and the average value was taken.

3.4. Release study of CP from Au-PSH-CP and Au-PSH-CP-FA

Synthesis of gold nanoconjugates containing CP and FA (Au-PSH-CP and Au-PSH-CP-FA) has been already discussed before. The nanoconjugates loose pellets obtained after centrifugation at 40,000 rpm at 10 °C for 1h in a Beckman TL-100 ultracentrifuge using a

TLA-100.2 rotor were divided into several fractions for analysis at different time points from 0 min to 24h. Each fraction was diluted with equal amount of PBS and incubated for 0, 5, 10, 15, 30 minutes and for 1, 2, 4 24 h at room temperature. After incubation with PBS, nanoconjugates were centrifuged at 40,000 rpm at 10 °C for 1h. The clear supernatants and loose pellets were collected and CP content analyzed by ICP-MS.

3.5. Release study of ^{3}H-FA from Au-PSH-CP-FA

Synthesis of gold nanoconjugates containing CP and FA (Au-PSH-CP-^{3}FA) has been already discussed before. The loose pellets obtained after centrifugation were divided into several fractions for analysis of ^{3}H-FA at different time points from 0 min to 24 h as discussed before. Each fraction was diluted with equal amount of PBS as indicated before and incubated for a defined time period as described above. After incubation, all fractions were further centrifuged at 40,000 rpm at 10 °C for 1 h. The clear supernatant and loose pellets were collected to measure the radioactivity by a scintillation counter to quantify the amount of FA released. Each experiment was repeated at least thrice.

3.7. Flow Cytometry of folate receptor

Cells (HUVECs, OSE, OVCAR-5 and OV-167) were grown in 100 mm tissue culture plates in their respective medium containing FBS to near confluency (~ 80%). Cells were then trypsinized, washed and counted followed by staining for 1 h on ice with a folate receptor alpha antibody (Alexis Pharmaceuticals, Cat. #804-439-R100) at a dilution of 1:100. After 1 h incubation with primary antibody, cells were washed thrice with PBS-BSA to remove excess primary antibody and incubated on ice for another 30 min with Alexa 488-conjugated anti-mouse secondary antibody. Finally, cells were washed thrice with PBS-BSA to remove excess secondary antibody and analyzed with a FACS Calibur flow cytometer (BD Biosciences, California).

4. RESULTS AND DISCUSSION

4.1. Physico-chemical Characterization

The as-synthesized AuNPs, obtained by the reduction of $HAuCl_4$ with $NaBH_4$, were characterized by UV-Visible spectroscopy and TEM. The evolution of a characteristic surface plasmon resonance (SPR) band in the visible region of the spectrum around 512 nm (λ_{max} =512 nm, Figure 1) suggested the formation of spherical gold nanoparticles.[15, 21, 22] Figure 1 demonstrates the change of absorption maxima (λ_{max}) of AuNPs upon additions of PSH-2k, CP and FA. Figure 1 clearly demonstrates a red shift in the SPR band maxima in Au-PSH (from λ_{max} = 512 nm to λ_{max} = 517 nm) upon the addition of PSH-2k compared to the spectrum of AuNPs alone (λ_{max} =512 nm). Similar red shifts in the λ_{max} values were also observed after the sequential addition of CP (Au-PSH-CP spectrum (λ_{max} =520 nm) and FA (Au-PSH-CP-FA spectrum (λ_{max} = 523 nm) to Au-PSH2 solution as compared with the spectrum of Au-PSH2 and AuNPs alone. The red shifts in the λ_{max} values upon addition of PSH2, CP and FA suggest the interaction and binding of the individual components with AuNP. Previously, we demonstrated the fabrication of a gold nanoconjugates containing FA through the intermediate layers of different PEG backbones such as PEG-tetramine-20K, PEG-diamine-10K, PEG-diamine-2K.[15] We further demonstrated that PEG-tetramine-20K was most effective spacer to attach FA to AuNP via electrostatic interaction and demonstrated their ability to target cancer cells. Similar attempts to fabricate a gold nanoconjugate containing, PEG-tetramines, CP and FA resulted in complete aggregation of the gold nanoparticles. Thus to avoid aggregation, we used sequential incubation process to first partially protect the nanogold surface with PSH2-2K and then added CP and FA. We speculate similar mechanism of interaction of FA with Au-PSH2-CP as described previously.[15]

The formation of AuNPs and its size was further confirmed by transmission electron microscopy (TEM). As previously reported, the TEM picture confirms that the size of unmodified AuNP synthesized by borohydride reduction method is ~ 5nm (data not shown). No significant aggregation of AuNPs was observed upon the addition of PSH2 and CP. Figures 2a and 2b exhibit the TEM micrographs of Au-PSH2 and Au-PSH2-CP. The micrographs clearly demonstrate that there is no significant aggregation of the nanoparticles upon the formation of Au-PSH2 or Au-PSH2-CP. Similarly, no significant aggregation was observed in Au-PSH2-CP-FA (data not shown).

It is previously reported that poly-ethylene glycol (PEG) backbones containing free-NH_2 or-SH functional group such as PAM2-2k(PEG-$(AM)_2$ 2000), PAM2-10k(PEG-$(AM)_2$ 10,000), PAM4-20k[(PEG-$AM)_4$ 20,000] and PSH2-2k [PEG-$(SH)_2$ 2000) have the ability to attach FA to AuNPs through noncovalent interaction. This interaction is dependent on the nature and number of reactive functional groups present in the PEG backbone.[15] As described previously Au-PAM4-20k led to the maximum attachment of ^{3}H-FA to AuNP via non-covalent interaction (~90%), whereas Au-PSH2-2k resulted in minimum attachment of ^{3}H-FA (~5%). As discussed above that the attempts to synthesize an AuNP based nanoconstructs containing PEG-amines, CP and FA led to complete aggregation of nanoparticles, whereas no such aggregation was found when PSH2-2k and CP were used in the construct. Thus, we chose to use thiol terminated PEGs rather than amine-terminated PEGs in the nanoconstruct. Furthermore, the presence of CP in the nanoconstruct along with PSH2-2k led to increased binding of FA, probably through non-covalent interaction. This is supported by the release profile of FA from different constructs as discussed below.

4.2. Release Profile of FA from the nanoconstruct

Release studies of FA and CP from the nanoconstruct provide useful insight on the mechanism of bonding of CP and FA to the nanoparticles. Therefore, it is very important to study the release profile of (i) CP in Au-PSH-CP and Au-PSH-CP-FA and (ii) release profile of ^{3}H-FA in Au-PSH-CP-FA nanoconjugates. 15, [16] The nanoconstruct fabrication and characterization is already described above and release studies were performed under physiological salt concentration, i.e. in PBS. The direct evidence for the attachment of CP to surface modified gold nanoparticles (Au-PSH) comes from the determination of platinum content using ICP-MS. ICP-MS demonstrates that nearly 50 % of CP used originally to synthesize Au-PSH-CP was bound to the nanoconjugate.

Another evidence for the attachment of CP to surface modified gold nanoparticles (Au-PSH) comes from the release profile of CP from gold nanoconjugates (Au-PSH-CP and Au-PSH-CP-FA) as described below. We have calculated the % of CP attachment to Au-PSH-CP and Au-PSH-CP-FA from the distribution of Pt content in the pellet and supernatant. Figure 3a represents the *in vitro* release profiles of CP from Au-PSH-CP nanoconjugates over time (0 min to 24 h) in PBS at room temperature. The figure demonstrates that only 8-10 % of CP is released up to 2 h incubation whereas it increased up to~ 12 % after 24 h incubation, demonstrating strong interaction of CP with Au-PSH2 and sufficient stability of Au-PSH-CP nanoconjugates in PBS.

In order to find out the stability of Au-PSH-CP-FA, we have carried out the *in vitro* release profiles of CP from Au-PSH-CP-FA nanoconjugates over time (0 min to 24 h) in PBS at room temperature (Figure 3b). The figure demonstrates that ~ 15 % of CP is released up to 1 h of incubation in PBS whereas it is increased up to 19 % after 24 h incubation, supporting sufficient stability of Au-PSH- CP-FA nanoconjugates. The relatively enhanced release of CP from Au-PSH2-CP-FA as compared to Au-PSH2-CP is not clear, but a possibility is that the incorporation of FA displaces some of the CP from the core of Au-PSH2-CP-FA.

It is also important to determine the attachment and the nature of bonding of FA to Au-PSH-CP-FA nanoconjugates. The evidence for the attachment of ^{3}H-FA to gold nanoparticles comes from the UV-visible spectroscopy as discussed earlier as well as from the release profile of ^{3}H-FA from gold nanoconjugates (Au-PSH-CP-^{3}H-FA) as described below. Synthesis of gold nanoconjugates containing CP and ^{3}H-FA (instead of FA) (Au-PSH-CP-^{3}H-FA) has been already discussed above. Radioactivity measurement in a scintillation counter was used to determine the amount of ^{3}H-FA in goldnanoconjugates (Au-PSH-CP-^{3}H-FA). It was also used to study the release profile of ^{3}H-FA in PBS from the conjugates. Figure 4 describes the release profile of ^{3}H-FA from Au-PSH-CP-^{3}H-FA over time (0 min to 24 h) in PBS at RT. It is evident from the figure that 17 % of ^{3}H-FA is released in supernatant within 5 min incubation period. However release of ^{3}H-FA is slowly increased from 21 % (at 10 min) to 52% (at 24h) over time. Thus, ~50% of ^{3}H-FA was still bound to the gold nanoconjugates even after 24 h incubation, supporting sufficient stability of Au-PSH-CP-^{3}H-FA.

The release profile of folic acid also provides important insight into the mechanism of bonding of FA to the nanoconstruct. The nature of the release profile of ^{3}H-FA in Au-PSH-CP-^{3}H-FA nanoconjugates is significantly different than that of ^{3}H-FA in Au-PSH-^{3}H-FA conjugates as reported previously.[15] Previously, we demonstrated that the release of ^{3}H-FA in Au-PSH-^{3}H-FA is rapid and nearly 90% was released within 24 h of incubation in PBS, possibly due to weak electrostatic interaction generated by PSH2-2k towards FA. However, in the current study we have demonstrated ~50% attachment of ^{3}H-FA in Au-PSH-CP-^{3}H-FA nanoconjugates even after 24 h of incubation. These results support that the presence of CP in the nanoconstruct confers stronger interaction of Au-PSH2-CP with FA leading to stronger stability and slower release of folic acid. Furthermore, it is also important to note that all the proliferation experiments with the cell lines were performed in their full media supplemented with 10-20 % serum. Even under such environments Au-PSH-CP-FA have been able to differentiate between normal cells and malignant cells whereas Au-PSH-CP could not. These results suggest that these conjugates are also stable in the presence of serum proteins. However, we speculate that there are possibilities that these conjugates will dissociate under endosomal/lysosomal acidic environment and in the presence of high intracellular GSH concentration.[23, 24]

Since the nanoconstruct contains FA, so we wanted to investigate its application in FR positive ovarian cancer cells. Hence, we determine the FR expression in different cancer cells such as OV167, OVCAR-5 and normal cells such as OSE and HUVEC. The procedure for the determination FR expression using fluorescence-activated cell sorting (FACS) using an N-terminal monoclonal antibody to FR-α has been already described in the method section above. The FR expression of HUVEC, OSE and OV-167 is presented in Figure 5. The figure demonstrates that among OV167, HUVEC and OSE, the FR expression pattern of these cells follow the order: OV-167 (92.1%)>HUVEC (9.9%)>OSE (2%).

4.3. Biological functional characterization

Finally, it is important to test the functional activity of CP in gold nanoconjugates (Au-PSH-CP-FA). The functional activity of CP in the nanoconstruct was tested against the proliferation of different cell lines *in vitro*. Proliferation experiments using ^{3}H-Thymidine are described in the materials and methods section. To find out the effect of Au-PSH-CP and Au-PSH-CP-FA on normal cells such as OSE and HUVECs ^{3}H-thymidine incorporation assay was performed as described in the materials and methods section. Cells were treated with different doses of the nanoconjugates (1-10 μM with respect to CP) for 72 h and the proliferation assay was performed. Figure 6a demonstrates the dose dependent effect of CP, Au-PSH-CP and Au-PSH-CP-FA on HUVEC cells. A significant dose dependent inhibition of proliferation (~ 40 %) was observed when cells were treated with free CP. Interestingly, no significant inhibition of

proliferation was observed when HUVECs were treated with CP either as Au-PSH2-CP or Au-PSH-CP-FA.

Similarly, dose dependent effects of CP, Au-PSH-CP and Au-PSH-CP-FA on OSE were demonstrated in figure 6b. It is evident from the figure that CP either as free CP or as in Au-PSH-CP significantly inhibited the proliferation of OSE (~ 70 %), whereas same dose of CP in the form of Au-PSH2-CP-FA protects the cytotoxic behavior of CP towards OSE cells. Lower cytotoxic insult of CP towards normal cells in nanoconjugated form, particularly, in the presence of FA is highly significant. The mechanism of such a unique behavior of CP is currently under investigation, but this form of delivery may resolve the core side effect issues associated with anti-cancer therapy.

The functional activity of CP in Au-PSH-CP and Au-PSH-CP-FA has been demonstrated against two ovarian cells, namely OVCAR-5 and OV-167 in a dose (1-10 μM) and time (24 - 72 h) dependent manner (Figure 7). Figure 7a demonstrates that CP, either free or nanoconjugated as in Au-PSH-CP and Au-PSH-CP-FA exhibits time dependent effect on the inhibition of proliferation, maximum inhibition being observed at the longest time point (72 h). Figure 7b demonstrates the dose dependent inhibition of proliferation of OVCAR-5 cells at different concentrations (0-10 μM) at 72h. It is evident from this figure that a dose dependent inhibition of proliferation was observed, maximum inhibition (~ 80 %) being at 10 μM for all treatment groups (CP, Au-PSH-CP and Au-PSH-CP-FA). It is also important to note that there is no significant difference in efficacy between free CP and Au-PSH-CP-FA, however, Au-PSH-CP demonstrating lower efficacy than free CP and Au-PSH-CP-FA.

A time and dose dependent effect of CP on OV-167 cells, either as a free drug or as a nanoconjugated drug was demonstrated in Figure 7c and 7d respectively. The figure clearly demonstrates that CP in Au-PSH-CP and Au-PSH-CP-FA exhibits time dependent effect on the inhibition of proliferation, while free CP (non-conjugated) does exhibit any time dependency (Figure 8c). Maximum inhibition was observed at the longest time point (72 h). Figure 8d demonstrates the effect of doses of CP either as a free drug or nanoconjugated drug to inhibit the proliferation of OV-167 cells. A dose dependent inhibition of proliferation was observed by CP treatment either as a free drug or as a nanoconjugated drug, maximum inhibition being observed at the highest dose (10 μM). However, Au-PSH-CP is demonstrating a protective effect on the cytotoxic insult of CP to both OVCAR-5 and OV-167 cells. The cause of this protective influence is interesting and a subject of future investigation.

Biological functional characterization of CP either as a free drug or as a nanoconjugated drug demonstrates that CP retains its cytotoxicity in nanoconjugated form. Interestingly, nanocnjugation in the form of Au-PSH-CP-FA protects the cytotoxic effect of CP to normal cells while enhancing cytotoxic effects to tumor cells. Although the mechanism of such an effect is currently under investigation, but this discovery is highly significant because this form of delivery may overcome the core issues of side effects of anti-cancer drugs.

5. CONCLUSION

This paper demonstrates the fabrication and functional characterization of a gold nanoparticle based drug delivery system. The nanoconstruct was characterized by UV-Vis spectroscopy, TEM microscopy and ICP-MS analysis demonstrating successful fabrication of the delivery system containing cis-Platin, folic acid and PEGs on a gold surface. Biological functional characterization demonstrates that Au-PSH-CP-FA not only retains the cytotoxic effect of CP, but it protects the normal cells from the cytotoxic insult of CP, while enhancing its cytotoxic effect towards the tumor cells. This type of behavior of CP in the nanoconjuagted form, specially in the form of Au-PSH-CP-FA is unique and currently under investigation. But this

form of delivery raises the possibility of overcoming the side effects of anti-cancer drug. In future, this methodology may be utilized for potential therapeutic application in ovarian cancer.

Supplementary Material

Refer to Web version on PubMed Central for supplementary material.

Acknowledgments

This work is supported by R01CA135011 and R01CA136494 to PM.

Reference

1. Zeisser-Labouebe M, Lange N, Gurny R, Delie F. Int. J. Pharm 2006;326:174–181. [PubMed: 16930882]
2. Jemal A, Murray T, Ward E, Samuels A. Ca-a Cancer J. Clin 2005;55:259–259.
3. Leffers N, Gooden MJM, de Jong RA, Hoogeboom BN, ten Hoor KA, Hollema H, Boezen HM, van der Zee AGJ, Daemen T, Nijman HW. Cancer Immunol. Immunother 2009;58:449–459. [PubMed: 18791714]
4. Kesterson J, Chan JK, Tian C, Monk BJ, Bell JG. Gynecol. Oncol 2009;112:S36–S37.
5. Vergote IB, Trimbos BJ, Guthrie D, Parmar M, Bolis G, Mangioni C, Anastasopolou A, Torri V, Vermorken J. Proc. Am. Soc. Clin. Oncol 2001;20:201a.
6. Goff BA, Mandel L, Muntz HG, Melancon CH. Cancer 2000;89:2068–2075. [PubMed: 11066047]
7. Kelemen LE, Sellers TA, Keeney GL, Lingle WL. Cancer Epidemiol. Biomarkers & Prev 2005;14:2168–2172.
8. Hasegawa K, Nakamura T, Harvey M, Ikeda Y, Oberg A, Figini M, Canevari S, Hartmann LC a, Peng KW. Clin.Cancer Res 2006;12:6170–6178. [PubMed: 17062694]
9. Low PS, Antony AC. Adv. Drug Delivery Rev 2004;56:1055–1238.
10. Reddy JA, Low PS. Crit. Rev. Ther. Drug Carrier Syst 1998;15:587–627. [PubMed: 9883391]
11. Parker N, Turk MJ, Westrick E, Lewis JD, Low PS, Leamon CP. Anal. Biochem 2005;338:284–293. [PubMed: 15745749]
12. Ni S, Stephenson SM, Lee RJ. Anticancer Res 2002;22:2131–2135. [PubMed: 12174894]
13. Leamon CP, Low PS. Drug Discov. Today 2001;6:44–51. [PubMed: 11165172]
14. Lu YJ, Low PS. Adv. Drug Delivery Rev 2002;54:675–693.
15. Bhattacharya R, Patra CR, Earl A, Wang S, Katarya A, Lu L, Kizhakkedathu JN, Yaszemski MJ, Greipp PR, Mukhopadhyay D, Mukherjee P. Nanomed 2007;3:224–238.
16. Patra CR, Bhattacharya R, Wang E, Katarya A, Lau JS, Dutta S, Muders M, Wang S, Buhrow SA, Safgren SL, Yaszemski MJ, Reid JM, Ames MM, Mukherjee P, Mukhopadhyay D. Cancer Res 2008;68:1970–1978. [PubMed: 18339879]
17. Mukherjee P, Bhattacharya R, Wang P, Wang L, Basu S, Nagy JA, Atala A, Mukhopadhyay D, Soker S. Clin. Cancer Res 2005;11:3530–3534. [PubMed: 15867256]
18. Mukherjee P, Bhattacharya R, Bone N, Lee YK, Patra CR, Wang S, Lu L, Secreto C, Banerjee PC, Yaszemski MJ, Kay NE, Mukhopadhyay D. J. Nanobiotechnology 2007;5:4. [PubMed: 17488514]
19. McDowell EM, Trump BF. Arch. Path. Lab. Med. 1976;10:405–414.
20. Spurr AR. J. Ultrastruct. Res 1969;26:31–36. [PubMed: 4887011]
21. Bhattacharya R, Patra CR, Verma R, Kumar S, Greipp PR, Mukherjee P. Adv. Mater 2007;19:711–716.
22. Daniel MC, Astruc D. Chem Rev 2004;104:293–346. [PubMed: 14719978]
23. Patra CR, Cao S, Safgren S, Bhattacharya R, Ames MM, Shah V, Reid JM, Mukherjee P. J. Biomed. Nanotech. 2008;4:508–14.
24. Hong R, Han G, Fernández JM, Kim BJ, Forbes NS, Rotello VM. J. Am. Chem. Soc. 2006;128(4):1078–9.

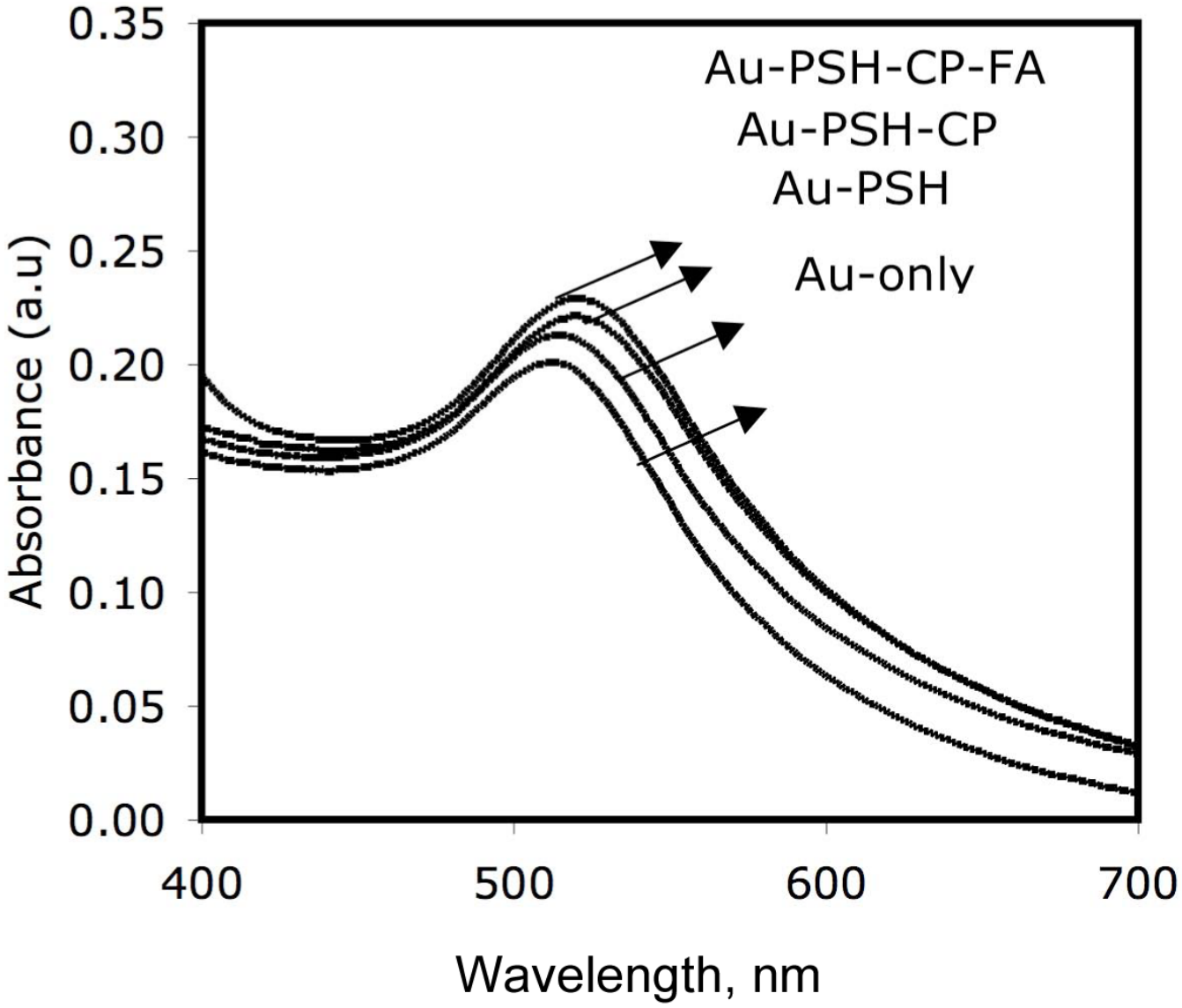

Fig.1.

UV-visible spectra of AuNPs, and gold nanocnjugates with (a) PEG-SH-2k (Au-PSH), (b) PEG-SH-2k & CP (Au-PSH-CP) and (c) PEG-SH-2k, CP and FA (Au-PSH-CP-FA). Change of absorption spectra of AuNPs as well as change of λ_{max} (towards red shift) upon the addition of PSH2-2k, CP and FA on AuNPs indicates the association of these molecules to AuNPs.

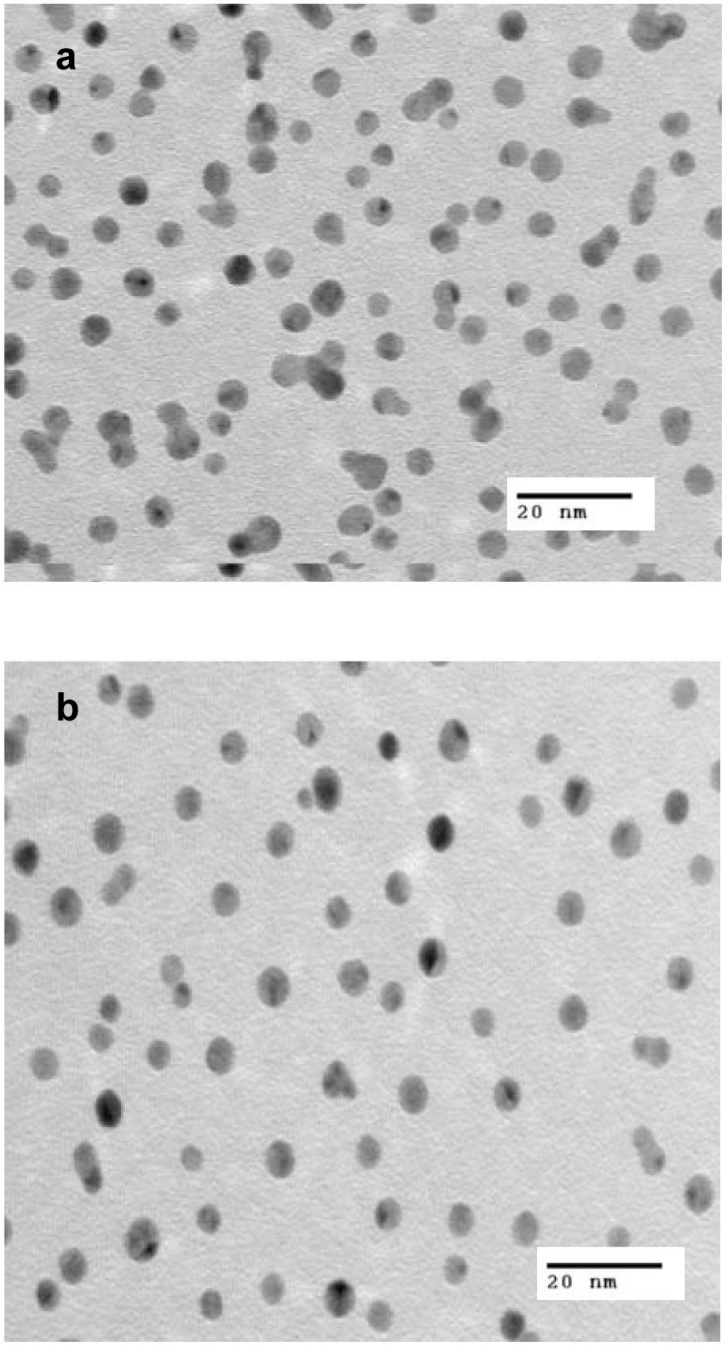

Figure 2.
Transmission electron images of (2a) Au-PSH-CP and (2b) Au-PSH-CP-FA shows there is no aggregation of AuNPs upon the addition Peg-SH-2k, CP and FA.

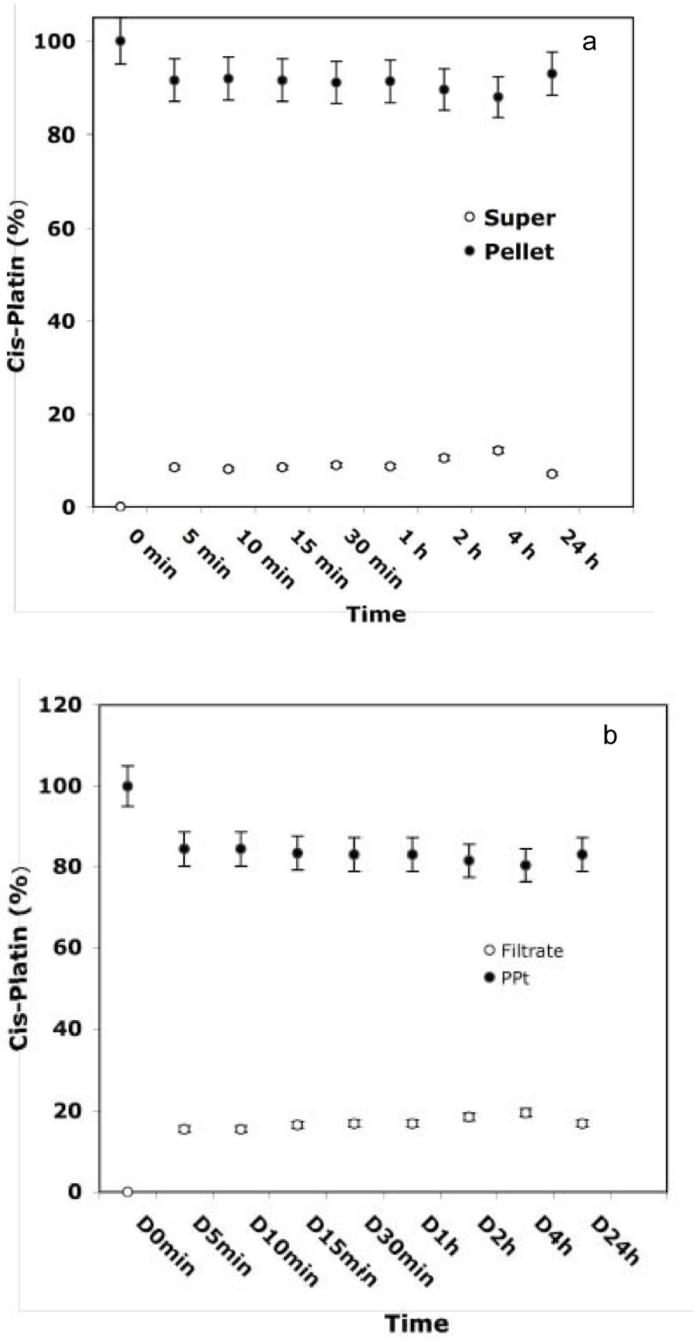

Figure 3.

Attachment and release profile of CP from purified gold nanoconjugates (Au-PSH-CP and Au-PSH-CP-FA) in PBS at room temperature with different time points (0-24h). Figures 3a and 3b describes the release of CP from Au-PSH-CP and Au-PSH-CP-FA, respectively. The amount of CP released in the supernatant was measured by ICP-MS analysis.

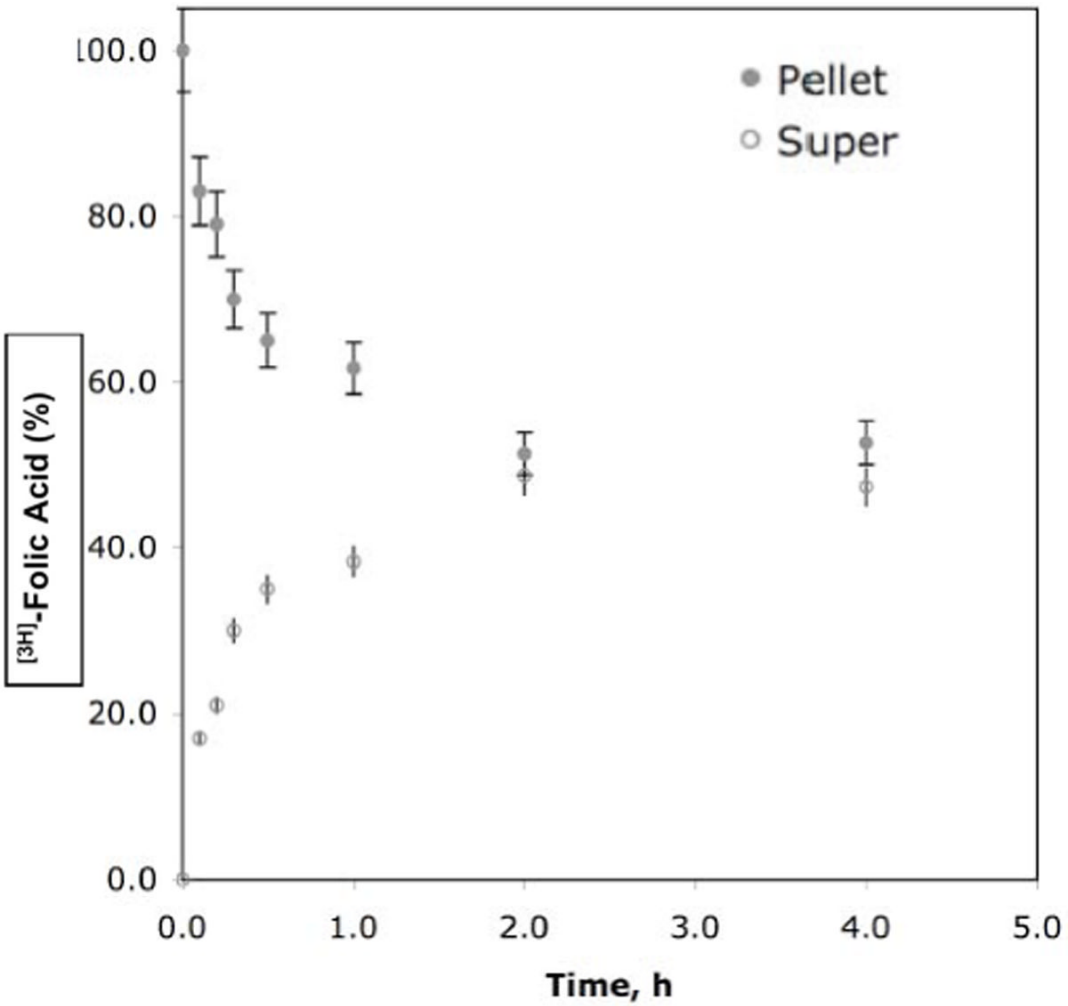

Figure 4.

Attachment and release profile of ^{3}H-FA from purified gold nanoconjugates (Au-PSH-CP-FA) in PBS at room temperature with different time points. The amount of folic acid released in the supernatant was measured by radioactivity in a scintillation counter.

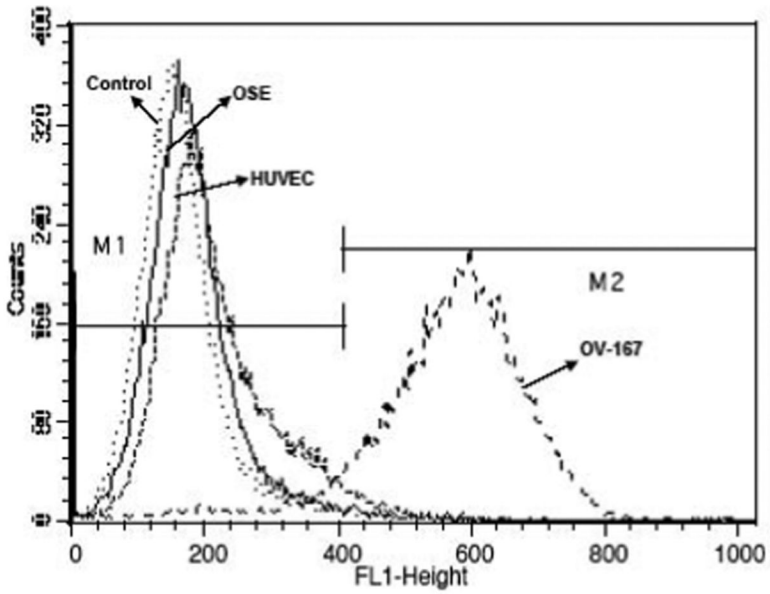

Figure 5.
The folate receptor (FR) expression in normal endothelial cells (HUVEC), normal ovarian surface epithelial (OSE) cells and in ovarian cancer cells (OV-167), observed by flow cytometry analysis.

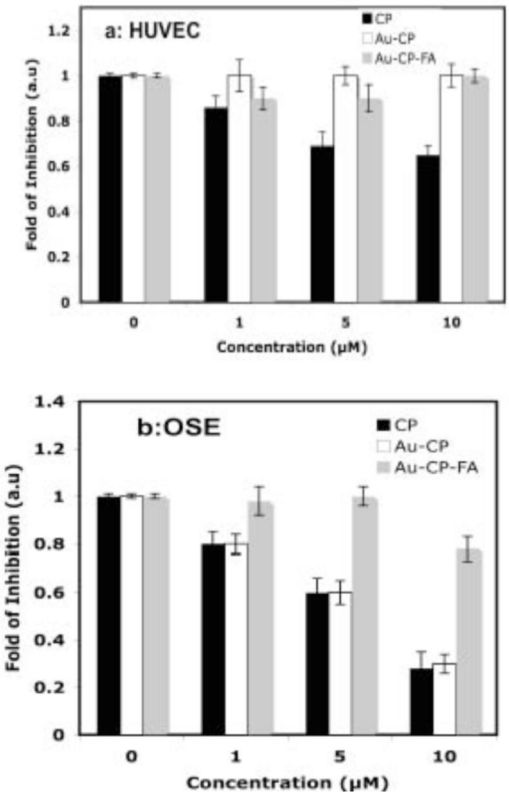

Figure 6.

Effect of free CP, and gold nanoconjugates (Au-PSH-CP & Au-PSH-CP-FA) on (a) normal endothelial cells (HUVEC) and (b) normal ovarian surface epithelial cells at a particular time (72 h) with different concentrations (1-10 μM), observed by [^{3}H]thymidine incorporation (cell proliferation) assay, presented as fold of inhibition. CP and other gold nanoconjugates, were added to HUVEC already starved with (0.1% serum) for 24 hours in 24-well plates and incubated for 2 hours and washed with PBS and replaced with fresh starved media then it was allowed to incubate for 72h. After 72 hours of incubation, 1 μCi [^{3}H]-thymidine was added into each well. Four hours later, cells were washed with cold PBS, fixed with 100% cold methanol, and collected for the measurement of trichloroacetic acid–precipitable radioactivity. Experiments were repeated in triplicate. The results show the non-toxic behavior of gold nanoconjugates.

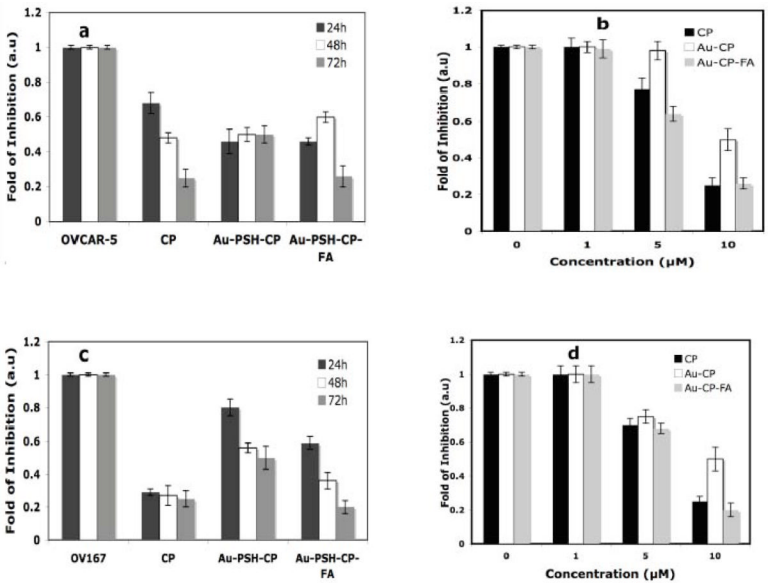

Figure 7.

In vitro efficacy of free CP, and gold nanoconjugates (Au-PSH-CP & Au-PSH-CP-FA) on ovarian cancer cells (OVCAR-5) with different times (24h, 48h and 72h, Figure 7a,) and doses (1-10 μM, Figure 7b), observed by [^{3}H]thymidine incorporation (cell proliferation) assay, presented as fold of inhibition. CP and other gold nanoconjugates, were added to OVCAR-5 for 24 hours in 24-well plates and incubated for 2 hours and washed with PBS and replaced with fresh complete media then it was allowed to incubate for different times (24-72h). After 24, 48 and 72 hours of incubation, 1 μCi [^{3}H]-thymidine was added into each well. Four hours later, cells were washed with cold PBS, fixed with 100% cold methanol, and collected for the measurement of trichloroacetic acid–precipitable radioactivity. Experiments were repeated in triplicate. The average data were obtained after performing the separate experiments in triplicate. Similarly, figures 7c and 7d demonstrates the time and dose dependent inhibition of proliferation of OV-167 cells either by free or nanoconjugated CP.